Available online at www.sciencedirect.com
ScienceDirect
Chaos, Solitons and Fractals 32 (2007) 862–882
CHAOS SOLITONS & FRACTALS
www.elsevier.com/locate/chaos

Nonlinear dynamics and strange attractors in the biological system

H.G. Enjieu Kadji [a,b], J.B. Chabi Orou [b], R. Yamapi [c,*], P. Woafo [a]

[a] *Laboratory of Nonlinear Modelling and Simulation in Engineering and Biological Physics, Faculty of Science, University of Yaounde I, P.O. Box 812, Yaounde, Cameroon*
[b] *Institut de Mathématiques et de Sciences Physiques, BP 613, Porto-Novo, Bénin*
[c] *Department of Physics, Faculty of Science, University of Douala, P.O. Box 24157, Douala, Cameroon*

Accepted 11 November 2005

Abstract

This paper deals with the nonlinear dynamics of the biological system modeled by the multi-limit cycles Van der Pol oscillator. Both the autonomous and non-autonomous cases are considered using the analytical and numerical methods. In the autonomous state, the model displays phenomenon of birhythmicity while the harmonic oscillations with their corresponding stability boundaries are tackled in the non-autonomous case. Conditions under which superharmonic, subharmonic and chaotic oscillations occur in the model are also investigated. The analytical results are validated and supplemented by the results of numerical simulations.

1. Introduction

Nonlinear oscillators have been a subject of particular interest in recent years [1–9]. This is due to their importance in many scientific fields ranging from physics, chemistry, biology to engineering. Among these nonlinear oscillators, a particular class contains self-sustained components such as the classical Van der Pol oscillator which serves as a paradigm for smoothly oscillating limit cycle or relaxation oscillations [3]. In the presence of an external sinusoidal excitation, it leads to various interesting phenomena such as harmonic, subharmonic and superharmonic oscillations, frequency entrainment [4], devil's staircase in the behavior of the winding number [5], chaotic behavior in a small range of control parameters [5–7]. The generalization of the classical Van der Pol oscillator including cubic nonlinear term (so-called Duffing–Van der Pol or Van der Pol–Duffing oscillator) has also been investigated by Venkatesan et al. in Ref. [8]. They have shown that the model exhibits chaotic motion between two types of regular motion, namely periodic and quasi-periodic oscillations in the principal resonance region. They have also obtained a perturbative solution for the periodic oscillations and carried out a stability analysis of such solution to predict the Neimark bifurcation. In this paper, we consider another self-excited model namely a biological system based on the enzymes–substrates reactions in order

* Corresponding author. Tel.: +237 932 93 76; fax: +237 340 75 69.
E-mail addresses: henjieu@yahoo.com (H.G. Enjieu Kadji), jchabi@yahoo.fr (J.B. Chabi Orou), ryamapi@yahoo.fr (R. Yamapi), pwoafo@uycdc.uninet.cm (P. Woafo).

0960-0779/$ - see front matter © 2005 Elsevier Ltd. All rights reserved.
doi:10.1016/j.chaos.2005.11.063

to show up the behavior of such a system in the autonomous and non-autonomous states. The paper is organized as follows: in Section 2, we describe the biological model under consideration and derive the equations of motion. Section 3 deals with the harmonic oscillatory states of such a model in the autonomous and non-autonomous states using respectively the Lindsted's perturbation method [9] and the harmonic balance method [1]. The stability boundaries of the forced harmonic oscillations are investigated using the Floquet theory [1,4]. In Section 4, light is shed on the superharmonic and subharmonic oscillations using the multiple time scales method [1]. Strange attractors and transition from regular to chaotic oscillations are tackled in Section 5 through numerical simulations. Conclusion is given in Section 6.

2. Biological model and equations of motion

Coherent oscillations in biological systems are considered here through the case of an enzymatic substrate reaction with ferroelectric behavior in brain waves model [10]. The following suggestions made by Frohlich [11,12] are taken as a physical basis for a theoretical investigation.

- When metabolic energy is available, long-wavelength electric vibrations are very strongly and coherently excited in active biological system.
- Biological systems have metastable states with a very high electric polarization.

These long range interactions may lead to a selective transport of enzymes and thus, rather specific chemical reactions may become possible. For this survey, let us consider a population of enzyme molecules of which N are in the excited polar state and R are not excited. We assume that S is the number of substrate molecules. Both the enzymes and the substrate show long range selective interactions which tend to increase their level by influx. Each transition from the non-polar (or weakly polar) ground state of enzyme to the highly polar excited state leads to the chemical destruction of a substrate molecule. Additionally, there are also spontaneous transitions from the excited to the ground (or weakly polar) state. It is assumed that the rate of increase of the activated enzymes is proportional to their own concentration N, to the rate of the unexcited enzymes R and to the number of the substrate molecules S. Therefore the system can be described by a system of nonlinear differential equations as follows:

$$\frac{dN}{d\tau} = vNRS - \xi N, \tag{1}$$

$$\frac{dS}{d\tau} = \gamma S - vNRS, \tag{2}$$

$$\frac{dR}{d\tau} = \xi N - vNRS - \lambda(R - C). \tag{3}$$

v represents the strength of the nonlinear enzyme–substrate reaction, ξ the decay rate of excited enzymes to the ground (or weakly polar) state and γ the range attraction of the substrate particles due to the autocatalytic reactions. $\lambda(R - C)$ also comes from the long range interaction with C the equilibrium concentration of the unexcited enzymes molecules in the absence of the excited enzyme and substrate, i.e., when $N = S = 0$. One supposes that the equilibrium of the unexcited enzyme concentration is reached fastly in order to simplify the above nonlinear equations. Such a process is also called an adiabatic elimination of the fast variable. Thus both Eqs. (1) and (2) are reduced to the well-known Lotka–Voltera equations [13]

$$\frac{dN}{d\tau} = vCNS - \xi N, \tag{4}$$

$$\frac{dS}{d\tau} = \gamma S - vCNS. \tag{5}$$

The number of activated enzyme molecules N can be viewed here as the predator concentration and the substrate molecules S as the prey population. From Eqs. (4) and (5), we derive the two following steady states $(N_0, S_0) = (0, 0)$ and $(N_0, S_0) = \left(\frac{\gamma}{vC}, \frac{\xi}{vC}\right)$. Perturbing these activated enzymes and substrate molecules around the nontrivial steady state lead us to obtain the equations

$$\begin{aligned} \frac{d\varepsilon}{d\tau} &= \gamma\eta + vC\eta\varepsilon, \\ \frac{d\eta}{d\tau} &= -\xi\varepsilon - vC\eta\varepsilon, \end{aligned} \tag{6}$$

where ε and η are respectively the excess concentrations of activated enzymes and substrate molecules beyond their equilibrium values N_0 and S_0. From Frohlich ideas, we may suppose that in large regions of the system of proteins, substrates, ions and structured water are activated by the chemical energy available from substrate enzyme reactions. Thus, chemical oscillations in the number of substrate and activated enzyme molecules with a very low frequency $\sqrt{\xi\gamma}$ might be carried out around the equilibrium state [14]. This oscillation also represents an electric oscillation through the high dipole moment of the excited enzyme. The electric dipole moment of the excited enzyme is partially screened by the ions and the remaining polarization causes the system to display a tendency towards a ferroelectric instability. On the other hand, electric resistances against the system's tendency to become ferroelectric also have to be accounted for and thus, give a contribution $-\sigma^2 P$ viewed as a relaxation term. Assuming the macroscopic polarization P to be proportional to the time dependent number ε of the excited enzyme molecules, a nonlinear dielectric contribution is obtained and given as follows:

$$\frac{\mathrm{d}\varepsilon}{\mathrm{d}\tau} = (\kappa^2 \mathrm{e}^{-\Psi^2\varepsilon^2} - \sigma^2)\varepsilon. \tag{7}$$

Since an electrical field F interacts with the polarization, it is also important to include its effect which consists of an internal field due to thermal fluctuations and an externally applied field on the excited enzyme. F does not need to be an electrical field necessary and can also represents for example external chemical influences (e.g., an input or an output of enzyme molecules through the transport phenomena). Therefore, adding both the chemical and the dielectric contribution finally lead us to the set of equations

$$\begin{aligned} \frac{\mathrm{d}\varepsilon}{\mathrm{d}\tau} &= \gamma\eta + (\kappa^2 \mathrm{e}^{-\Psi^2\varepsilon^2} - \sigma^2)\varepsilon + vC\eta\varepsilon + F(\tau), \\ \frac{\mathrm{d}\eta}{\mathrm{d}\tau} &= -\xi\varepsilon - vC\eta\varepsilon. \end{aligned} \tag{8}$$

For small values of ε and η, if one considers the development in series of the function $\mathrm{e}^{-\Psi^2\varepsilon^2}$ at the third order to take into account the effects of some nonlinear quantities provided from the excess of concentration of the activated enzymes and uses the following rescaling:

$$\omega_0 = \sqrt{\xi\gamma}, \qquad t = \omega_0\tau, \qquad x = \Xi\varepsilon, \qquad \Xi = \sqrt{\frac{3}{\kappa^2 - \sigma^2}}\kappa\Psi, \qquad \mu = \frac{\kappa^2 - \sigma^2}{\omega_0},$$
$$E(t) = \frac{\Xi}{\omega_0^2}\frac{\mathrm{d}}{\mathrm{d}t}F\left(\frac{t}{\omega_0}\right), \qquad \alpha = \frac{5}{18\kappa^2}(\kappa^2 - \sigma^2), \qquad \beta = \frac{7}{162\kappa}(\kappa^2 - \sigma^2)^2,$$

one have that the biological system is governed by the coming equation

$$\ddot{x} - \mu(1 - x^2 + \alpha x^4 - \beta x^6)\dot{x} + x = E\cos\Omega t, \tag{9}$$

where an overdot denotes time derivative. The quantities α, β are positive parameters, μ is the parameter of nonlinearity while E and Ω are respectively the amplitude and the frequency of the external excitation. The biological system modeled through Eq. (9) has been considered by Kaiser in Ref. [15]. He has emphasized that in the unforced case, the model is a multi-limit cycles oscillator (so-called the multi-limit cycles Van der Pol oscillator (**MLC-VdPo**)). Since that model has been introduced, just few aspects of his dynamics have been analyzed. Indeed, Kaiser and Eichwald have investigated additionally to the dominating scenarios bifurcation in the superharmonic region [16], the occurrence of a symmetry breaking crisis subsequent type *III* intermittency [17]. Our aim is to tackle some aspects of its dynamics which remain unsolved, both in the autonomous and non-autonomous cases, using analytical methods and numerical simulations.

3. Harmonic oscillatory states

3.1. Autonomous oscillatory states

We consider in this subsection the case where the model is not influenced by an external force ($E = 0$) and our purpose is to find the amplitudes and frequencies of the limit cycles. Therefore, an appropriate analytical tool is the Lindsted's perturbation method [9]. In order to permit an interaction between the frequency and the amplitude, it is interesting to set $\tau = \omega t$ where ω is an unknown frequency. We assume that the periodic solution of Eq. (9) can be performed by an approximation having the form

$$x(\tau) = x_0(\tau) + \mu x_1(\tau) + \mu^2 x_2(\tau) + \cdots, \tag{10}$$

where the functions $x_n(\tau)$ $(n = 0, 1, 2, \ldots)$ are periodic functions of τ of period 2π. Moreover, the frequency ω can be represented by the following expression:

$$\omega = \omega_0 + \mu\omega_1 + \mu^2\omega_2 + \cdots, \tag{11}$$

where ω_n $(n = 0, 1, 2, \ldots)$ are unknown constants at this point. Substituting the expressions (10) and (11) in Eq. (9) and equating the coefficients of μ^0, μ^1 and μ^2 to zero, we obtain the following equations at different order of μ:

Order μ^0

$$\omega_0^2\ddot{x}_0 + x_0 = 0. \tag{12}$$

Order μ^1

$$\omega_0^2\ddot{x}_1 + x_1 = \omega_0(1 - x_0^2 + \alpha x_0^4 - \beta x_0^6)\dot{x}_0 - 2\omega_0\omega_1\ddot{x}_0 + \omega_0 x_0^4\dot{x}_0(\alpha - \beta x_0^2). \tag{13}$$

Order μ^2

$$\begin{aligned}\omega_0^2\ddot{x}_2 + x_2 = {} & \omega_0[(1 - x_0^2)\dot{x}_1 - 2x_0\dot{x}_0x_1] - 2\omega_0\omega_1\ddot{x}_1 - (\omega_1^2 + 2\omega_0\omega_2)\ddot{x}_0 - \omega_1(1 - x_0^2)\dot{x}_0 + \omega_1(\alpha - \beta x_0^2)x_0^4\dot{x}_1 \\ & + \omega_0[(\alpha - \beta x_0^2)x_0^4\dot{x}_1 + (4\alpha - 6\beta x_0^2)x_0^3\dot{x}_0x_1].\end{aligned} \tag{14}$$

Making use of the property $x(\tau + 2\pi) = x(\tau)$ and the initial condition $\dot{x}(0) = 0$ to determine the unknown quantities in the above equations, we get

$$x_n(\tau + 2\pi) = x_n(\tau); \quad \dot{x}_n(0) = 0; \quad n = 0, 1, 2. \tag{15}$$

Solving Eq. (12) and using conditions (15), it comes

$$x_0 = A\cos\tau, \tag{16}$$

$$\omega_0 = 1, \tag{17}$$

where A is the amplitude of the limit cycle. In virtue of the solution (16) and the relation (17), Eq. (13) leads to

$$\begin{aligned}\ddot{x}_1 + x_1 = {} & \left(\frac{5\beta}{64}A^6 - \frac{\alpha}{8}A^4 + \frac{1}{4}A^4 - 1\right)A\sin\tau + 2\omega_1 A\cos\tau + \left(\frac{9\beta}{64}A^7 - \frac{3\alpha}{16}A^5 + \frac{1}{4}A^3\right)\sin 3\tau \\ & + \left(\frac{5\beta}{64}A^7 - \frac{\alpha}{16}A^5\right)\sin 5\tau + \frac{\beta}{64}A^7\sin 7\tau.\end{aligned} \tag{18}$$

From this latter equation, the secularity conditions (so called the solvability conditions) lead us to the following:

$$\frac{5\beta}{64}A^6 - \frac{\alpha}{8}A^4 + \frac{1}{4}A^2 - 1 = 0, \tag{19}$$

and

$$\omega_1 = 0. \tag{20}$$

Thus, a general expression for a periodic solution of Eq. (18) can be written as follows:

$$x_1 = \Gamma\cos\tau + \Upsilon\sin\tau + \Psi_1\sin 3\tau + \Psi_2\sin 5\tau + \Psi_3\sin 7\tau, \tag{21}$$

where

$$\Psi_1 = -\frac{1}{32}\left(\frac{9\beta}{16}A^7 - \frac{3\alpha}{4} + A^3\right), \qquad \Psi_2 = -\frac{1}{384}\left(\frac{5\beta}{4} - \alpha A^5\right), \qquad \Psi_3 = -\frac{\beta}{3072}A^7$$

with the initial condition $\dot{x}_n(0)$, one now obtains

$$\Upsilon = \frac{219}{3072}\beta A^7 - \frac{1}{12}\alpha A^5 + \frac{3}{32}A^3.$$

The value of Γ remains undetermined for the moment and will be determined in the next step. The secularity condition for the solution $x_2(\tau)$ yields the following solutions:

$$\Gamma = 0, \tag{22}$$

and

$$\omega_2 = \frac{1580\beta}{393216}A^{12} - \frac{738\alpha\beta}{99024}A^{10} + \left(\frac{72\alpha^2 + 309\beta}{768}\right)A^8 - \left(\frac{64\alpha - 219\beta}{6144}\right)A^6 + \left(\frac{16\alpha + 3}{384}\right)A^4 - \frac{3}{64}A^2. \tag{23}$$

Therefore, the solution of Eq. (9) can be approximated by

$$x(t) = A\cos\omega t + \mu(\Upsilon\sin\omega t + \Psi_1\sin 3\omega t + \Psi_2\sin 5\omega t + \Psi_3\sin 7\omega t) + \mathrm{O}(\mu^2), \tag{24}$$

where the frequency ω is given by

$$\omega = 1 + \mu^2\omega_2 + \mathrm{O}(\mu^3). \tag{25}$$

The amplitudes A_n $(n = 1, 2, 3)$ of the limit cycles and their related frequencies $\omega(A_n)$ are obtained by solving respectively Eqs. (19) and (25) via the Newton–Raphson algorithm. Depending to the values of the parameters α and β, Eq. (19) can give birth to one or three positive amplitudes which correspond respectively to the amplitudes of one or three limit cycles. In the case of three limit cycles, two are stable and one is unstable. For instance, with $\alpha = 0.144$ and $\beta = 0.005$, the stable limit cycles have the following characteristics $A_1 = 2.6390$ with the frequency $\omega(A_1) = 1.0011$ and $A_2 = 4.8395$ with $\omega(A_2) = 1.0545$ while the unstable limit cycle is given by $A_3 = 3.9616$ with $\omega(A_3) = 1.0114$. Such a coexistence of two stable limit cycles with different amplitudes and frequencies (or periods) separated by an unstable limit cycle for a given set of parameters refer to as birhythmicity [18]. Therefore, birhythmicity provides the capability of switching back and forth, upon appropriate perturbation or parameter change, between two distinct types of stable oscillations characterized by markedly different periods (or frequencies) and amplitudes. Such a phenomenon is used to model glycotic oscillations in yeast and muscle [19,20]. The unstable limit cycle represents the separatrix between the basins of attraction of the two stable limit cycles. From Eq. (19), a map showing some regions where one or three limit cycles can be found has been constructed as shown in Fig. 1. The above stable limit cycles and their corresponding attraction basins are obtained from a direct numerical simulation of Eq. (9) using the fourth-order Runge–Kutta algorithm (see Fig. 2). The evolution of the amplitude of oscillations versus the parameter α for different values of the parameter β has also been drawn from Eq. (19) as shown in Fig. 3. It appears from that figure the occurrence of jump phenomenon which disappear with increasing β. Such situations can illustrate the explanation of the existence of multiple frequency

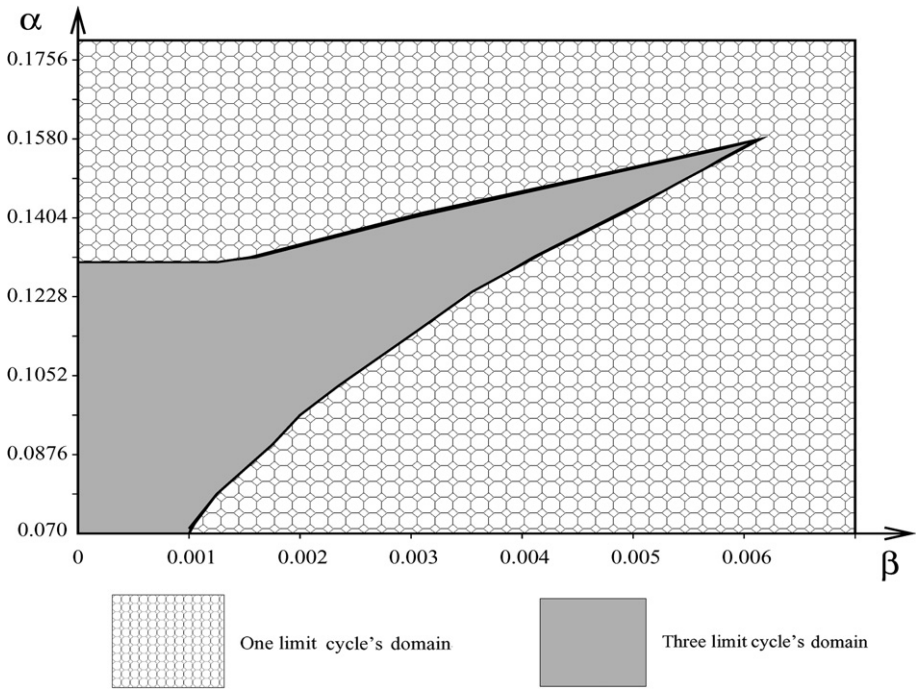

Fig. 1. A limit cycles map showing some regions where one or three limit cycles can be found.

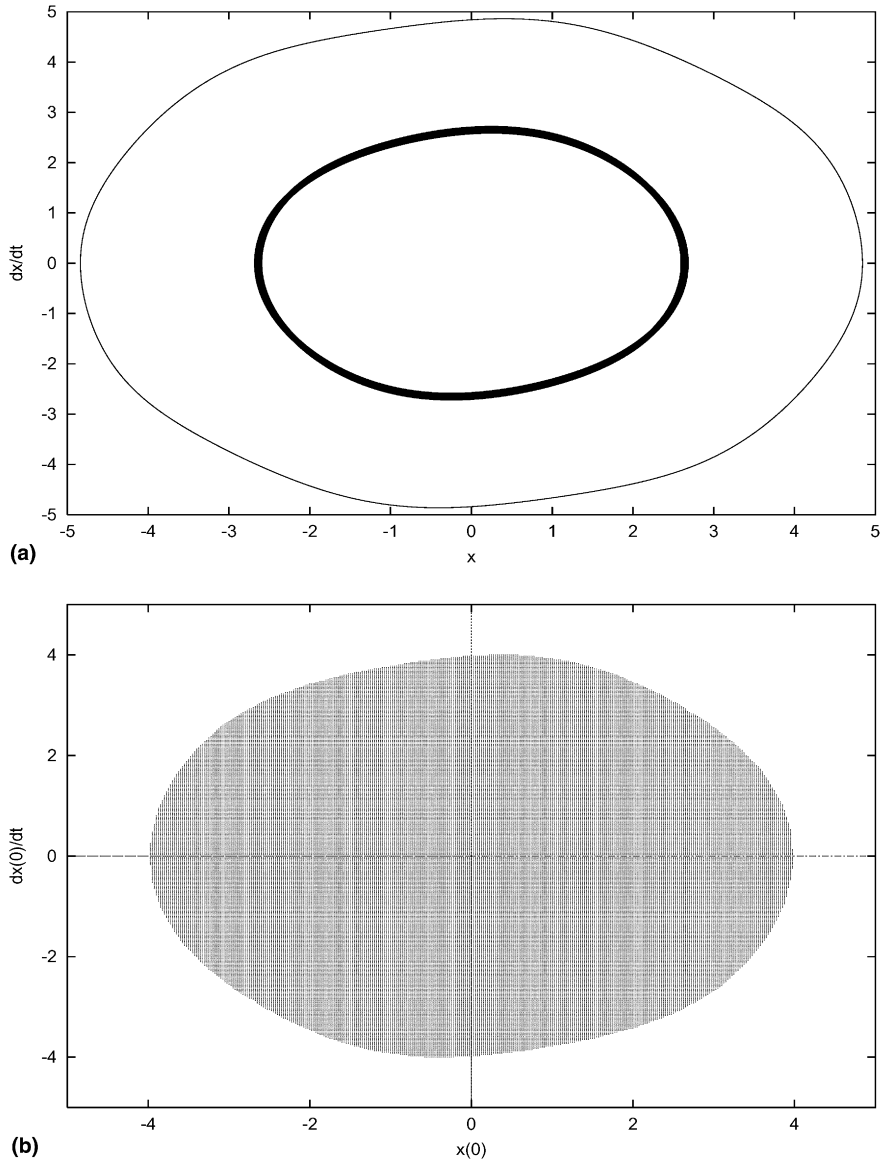

Fig. 2. Phases portrait of the two stable limit cycles (a) and their corresponding basins of attraction (b) for $\mu = 0.1$, $\alpha = 0.144$ and $\beta = 0.005$.

and intensity windows in the reaction of biological systems when they are irradiated with very low weakelectromagnetic fields [21–24].

3.2. Forced harmonic oscillatory states

3.2.1. Harmonic oscillatory states

Assuming that the fundamental component of the solutions has the period of the external excitation, we use the harmonic balance method [1] to derive the amplitude of the forced harmonic oscillatory states ($E \neq 0$) of Eq. (9). For this purpose, we express its solution x_s as

$$x_s = a_1 \cos \Omega t + a_2 \sin \Omega t. \tag{26}$$

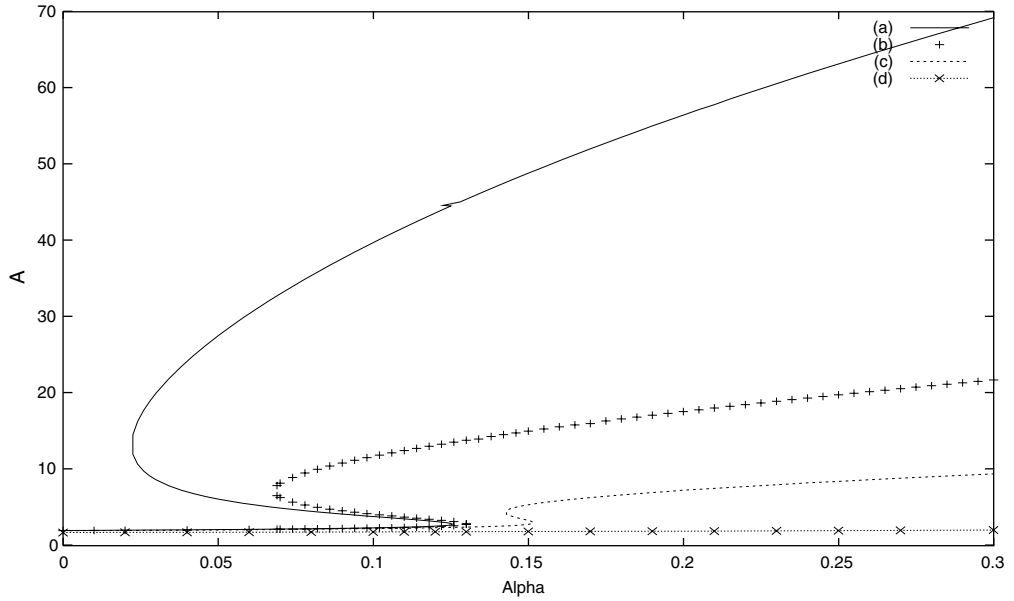

Fig. 3. Behavior of the amplitude of autonomous oscillatory states versus α for different values of β (a) $\beta = 10^{-4}$, (b) $\beta = 10^{-3}$, (c) $\beta = 5\times\ 10^{-3}$, (d) $\beta = 0.1$.

Inserting Eq. (26) in Eq. (9) and equating the cosine and sine terms separately, we obtain

$$\begin{aligned}(1-\Omega^2)a_1 - \mu\Omega\left(1-\frac{1}{4}A^2+\frac{\alpha\Omega}{8}A^4-\frac{5\beta}{64}A^6\right)a_2 = E,\\ \mu\Omega\left(1-\frac{1}{4}A^2+\frac{\alpha\Omega}{8}A^4-\frac{5\beta}{64}A^6\right)a_1 + (1-\Omega^2)a_2 = 0,\end{aligned} \tag{27}$$

where

$$A^2 = a_1^2 + a_2^2; \qquad \tan\phi = \frac{\mu\Omega(1-\frac{1}{4}A^2+\frac{\alpha\Omega}{8}A^4-\frac{5\beta}{64}A^6)}{\Omega^2-1}.$$

After some algebraic manipulations of Eq. (27), it comes that the amplitude A satisfies the following nonlinear algebraic equation:

$$\frac{25\beta^2}{4096}A^{14} - \frac{5\alpha\beta\Omega}{256}A^{12} + \left(\frac{2\alpha^2\Omega^2+5\beta}{128}\right)A^{10} - \left(\frac{2\alpha\Omega+5\beta}{32}\right)A^8 + \left(\frac{4\alpha\Omega+1}{16}\right)A^6 - \frac{1}{2}A^4 + \left(1+\frac{(1-\Omega^2)^2}{\mu^2\Omega^2}\right)A^2 - \frac{E^2}{\mu^2\Omega^2} = 0. \tag{28}$$

We find the behavior of A when the frequency of the external excitation Ω is varied and the results are represented in Fig. 4 where the comparison between analytical and numerical response frequency curves $A(\Omega)$ of the model is shown. We provide in Fig. 5 the effects of E on the multi-limit cycles and it appears that as soon as the amplitude of the external excitation is different from zero, one of the two stable limit-cycles collapses. The physiological importance of such a situation can be explained by the fact that the membrane has stored a lot of energy which created the destruction of one of the two stale limit cycles. The remaining stable limit cycle displays resonance peaks which disappears as the amplitude E increases for some range of parameters. The phenomenon of destruction of one of the two stable limit cycles under the effect of an external field is of capital importance in biology. It is for example the case where one of the cycles is a pathological cycle whereas the second is a physiological limit cycle. In such a situation, the destruction of the pathological limit cycle under the effects of E, which can be represented by external chemical influences (e.g., an input or an output of enzyme molecules via the transport phenomena) is of utility.

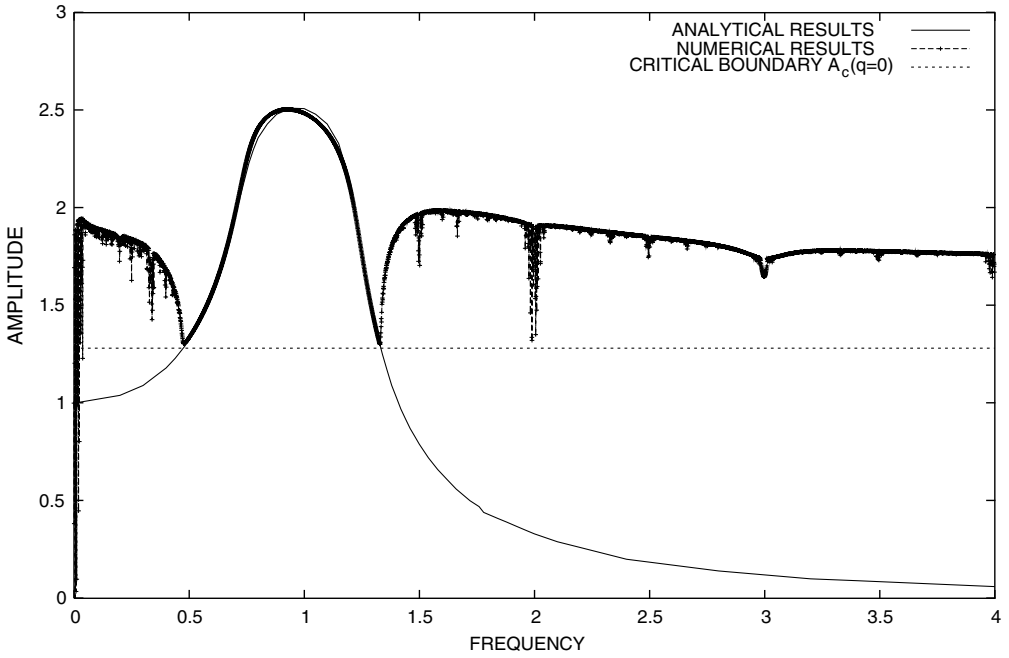

Fig. 4. Comparison between analytical and numerical frequency–response curve $A(\Omega)$ with the parameters $\alpha = 0.10$, $\beta = 0.2$, $\mu = 0.1$ and $E = 1.0$.

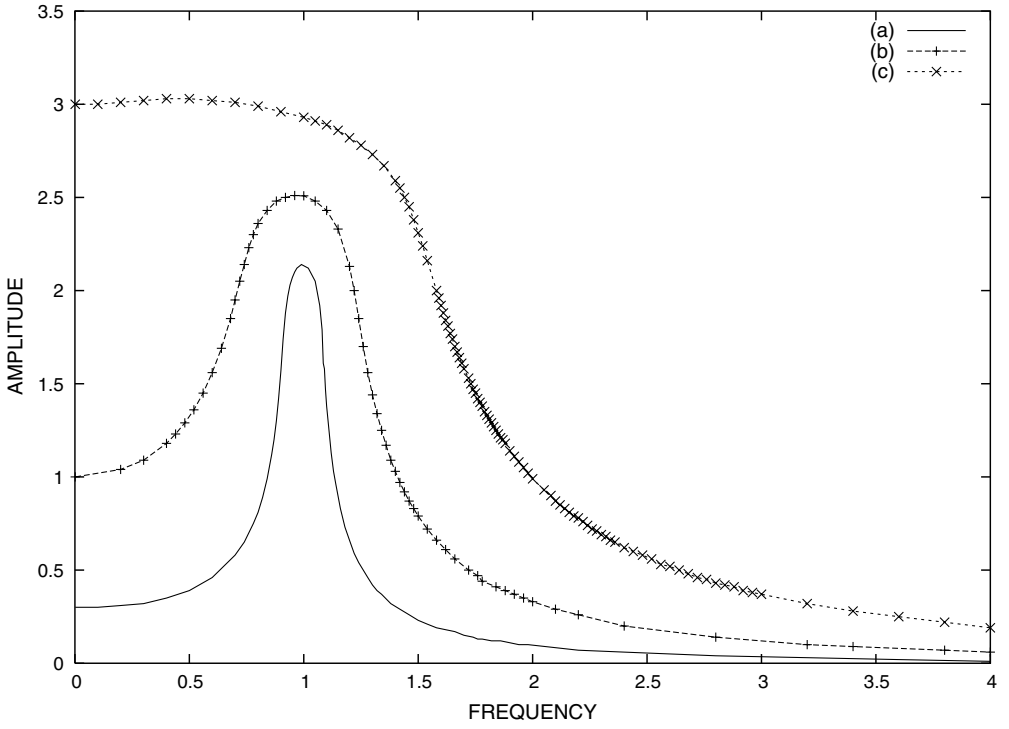

Fig. 5. Effects of the external excitation E on the amplitude of oscillations with the parameters of Fig. 4. (a) $E = 0.3$, (b) $E = 1.0$, (c) $E = 3.0$.

3.2.2. Stability of the harmonic oscillations

To examine local stability of the harmonic solution, we derive the linear variational equation from Eq. (9) around the oscillatory states and obtain

$$\ddot{\zeta} - \mu(1 - x_s^2 + \alpha x_s^4 - \beta x_s^6)\dot{\zeta} + [1 + \mu(2x_s - 4\alpha x_s^3 + 6\beta x_s^5)\dot{x}_s]\zeta = 0, \tag{29}$$

where x_s is the oscillatory states defined by Eq. (26). The oscillatory states are stable if ζ tends to zero when the time goes up. With regard to the evolution of the biological system represented by x_s, ζ can indicate an exogenic hormonal agent which forms the basis of the theurapeutic action. The therapy will consist to seek temporal laws to be followed by the exogenic hormone so that after a transitional phase, the state of the system remains more close to physiological behavior [25]. The appropriate analytical tool to examine the stability condition is the Floquet theory [1,4]. Setting $t = \frac{2\tau}{\Omega}$, the variational Eq. (29) can be rewritten as

$$\ddot{\zeta} + \Upsilon(\tau)\dot{\zeta} + \Gamma(\tau)\zeta = 0, \tag{30}$$

where

$$\Upsilon(\tau) = -\frac{2\mu}{\omega}[H + I\cos(4\tau - 2\phi) + J\cos(8\tau - 4\phi) + K\cos(12\tau - 6\phi)],$$
$$\Gamma(\tau) = \frac{4}{\omega^2}[1 + L\sin(4\tau - 2\phi) + M\sin(8\tau - 4\phi) + Q\sin(12\tau - 6\phi)],$$

with

$$H = 1 - \frac{1}{2}A^2 + \frac{3\alpha}{8}A^4 - \frac{5\beta}{16}A^6, \qquad I = -\frac{1}{2}A^2 + \frac{\alpha}{2}A^4 - \frac{15\beta}{32}A^6, \qquad J = \frac{\alpha}{8}A^4 - \frac{3\beta}{16}A^6, \qquad K = -\frac{\beta}{32}A^6,$$
$$L = -\mu\Omega A^2\left(2 + 2\alpha A^2 - \frac{15\beta}{8}A^4\right), \qquad M = \frac{\mu\Omega}{2}A^4\left(\alpha - \frac{3\beta}{2}A^2\right), \qquad Q = -\frac{3\mu\beta}{16}A^6.$$

To discuss further the stability process, we first transform Eq. (30) into the standard form by introducing a new variable Λ as follows:

$$\begin{aligned}\zeta(\tau) &= \Lambda(\tau)\exp\left\{-\frac{1}{2}\int_0^\tau \Upsilon(\tau')\,\mathrm{d}\tau'\right\} \\ &= \Lambda(\tau)\exp\left\{-q\tau + \frac{\mu}{4\omega}\left[I\sin(4\tau - 2\phi) + \frac{J}{2}\sin(8\tau - 4\phi) + \frac{K}{3}\sin(12\tau - 6\phi)\right]\right\},\end{aligned} \tag{31}$$

where

$$q = \frac{\mu}{\Omega}\left[\frac{5\beta}{16}A^6 - \frac{3\alpha}{8}A^4 + \frac{1}{2}A^2 - 1\right].$$

By coupling both Eqs. (30) and (31), it comes that Λ satisfies the following equation:

$$\begin{aligned}\ddot{\Lambda} + [&\kappa_0 + \kappa_{4c}\cos(4\tau - 2\phi) + \kappa_{4s}\sin(4\tau - 2\phi) + \kappa_{8c}\cos(8\tau - 4\phi) + \kappa_{8s}\sin(8\tau - 4\phi) + \kappa_{12c}\cos(12\tau - 6\phi) \\ &+ \kappa_{12s}\sin(12\tau - 6\phi) + \kappa_{16c}\cos(16\tau - 8\phi) + \kappa_{20c}\cos(20\tau - 10\phi) + \kappa_{24c}\cos(24\tau - 12\phi)]\Lambda = 0,\end{aligned} \tag{32}$$

with

$$\kappa_0 = \frac{1}{\Omega^2}\left[4 - \frac{\mu^2}{2}(2H^2 + I^2 + J^2 + K^2)\right], \qquad \kappa_{4c} = -\frac{\mu^2}{\Omega^2}(2HI + IJ + JK), \qquad \kappa_{4s} = \frac{4}{\Omega^2}(L - \mu\Omega I),$$
$$\kappa_{8c} = -\frac{\mu^2}{\Omega^2}\left(\frac{I^2}{2} + 2HJ + IK\right), \qquad \kappa_{8s} = \frac{4}{\Omega^2}(M - 2\mu\Omega I), \qquad \kappa_{12c} = -\frac{\mu^2}{\Omega^2}(2HK + IJ),$$
$$\kappa_{12s} = \frac{4}{\Omega^2}(N - 3\mu\Omega K), \qquad \kappa_{16c} = -\frac{\mu^2}{\Omega^2}\left(\frac{J^2}{2} + IK\right), \qquad \kappa_{20c} = -\frac{\mu^2}{\Omega^2}JK, \qquad \kappa_{24c} = -\frac{\mu^2}{2\Omega^2}K^2.$$

The Floquet theory [1,4] now leads us to seek a particular solution of Eq. (32) in the following form:

$$\Lambda = \exp(\epsilon\tau)\psi(\tau) = \sum_{n=-\infty}^{n=+\infty}\psi_n\exp(\epsilon_n\tau), \quad \epsilon_n = \epsilon + 2\mathrm{j}n, \tag{33}$$

where $\psi(\tau) = \psi(\tau + \pi)$ replaces the Fourier series and ϵ is the complex number while ϵ_n is a constant. Substituting Eq. (33) into Eq. (32) and equating each of the coefficients of exponential functions to zero yields the following homogeneous equation for ψ_m:

$$\begin{aligned}
&[\epsilon_m^2 + \kappa_0]\psi_m + \frac{1}{2}[\kappa_{4c} - \mathrm{j}\kappa_{4s}]\exp(-2\mathrm{j}\phi)\psi_{m-2} + \frac{1}{2}[\kappa_{4c} + \mathrm{j}\kappa_{4s}]\exp(2\mathrm{j}\phi)\psi_{m+2} + \frac{1}{2}[\kappa_{8c} - \mathrm{j}\kappa_{8s}]\exp(-4\mathrm{j}\phi)\psi_{m-4} \\
&+ \frac{1}{2}[\kappa_{8c} + \mathrm{j}\kappa_{8s}]\exp(4\mathrm{j}\phi)\psi_{m+4} + \frac{1}{2}[\kappa_{12c} - \mathrm{j}\kappa_{12s}]\exp(-6\mathrm{j}\phi)\psi_{m-6} + \frac{1}{2}[\kappa_{12c} + \mathrm{j}\kappa_{12s}]\exp(6\mathrm{j}\phi)\psi_{m+6} \\
&+ \frac{1}{2}\kappa_{16c}\exp(-8\mathrm{j}\phi)\psi_{m-8} + \frac{1}{2}\kappa_{16c}\exp(8\mathrm{j}\phi)\psi_{m+8} + \frac{1}{2}\kappa_{20c}\exp(-10\mathrm{j}\phi)\psi_{m-10} + \frac{1}{2}\kappa_{20c}\exp(10\mathrm{j}\phi)\psi_{m+10} \\
&+ \frac{1}{2}\kappa_{24c}\exp(-12\mathrm{j}\phi)\psi_{m-12} + \frac{1}{2}\kappa_{24c}\exp(12\mathrm{j}\phi)\psi_{m+12} = 0.
\end{aligned} \tag{34}$$

For nontrivial solutions, the determinant of the matrix in Eq. (34) must vanish. But since the determinant is infinite, convergence considerations are taking into account by dividing Eq. (34) by $\kappa_0 - 4m^2$. Considering only the central rows and columns of the Hill determinant [1], approximate solutions are obtained through the following approximate characteristic equation:

$$\Delta(\epsilon) = \begin{vmatrix} (\epsilon - 2\mathrm{j})^2 + \kappa_0 & 0 & \frac{1}{2}(\kappa_{4c} + \mathrm{j}\kappa_{4s})\exp(2\mathrm{j}\phi) \\ 0 & \epsilon^2 + \kappa_0 & 0 \\ \frac{1}{2}(\kappa_{4c} - \mathrm{j}\kappa_{4s})\exp(-2\mathrm{j}\phi) & 0 & (\epsilon + 2\mathrm{j})^2 + \kappa_0 \end{vmatrix} = 0, \tag{35}$$

or

$$(\epsilon^2 + \kappa_0)\left[\epsilon^4 + 2(\kappa_0 + 4)\epsilon^2 + (\kappa_0 - 4)^2 - \frac{1}{4}(\kappa_{4c}^2 + \kappa_{4s}^2)\right] = 0.$$

Since the characteristic exponents ϵ are the solutions of $\Delta(\epsilon) = 0$, there are three following possibilities of solutions as follows:

- $\epsilon = \pm\mathrm{j}\sqrt{\kappa_0}$,
- $\epsilon = \pm\mathrm{j}\sqrt{\kappa_0 + 4 + \sqrt{\Delta}}$,
- $\epsilon = \pm\sqrt{-(\kappa_0 + 4) + \sqrt{\Delta}}$,

where $\Delta = 16\kappa_0 + \frac{1}{4}(\kappa_{4c}^2 + \kappa_{4s}^2)$.

Once ϵ are known and either imaginary $\epsilon = \pm\mathrm{j}\bar{\epsilon}$ or real $\epsilon = \pm\bar{\epsilon}$ ($\bar{\epsilon}$ real positive). We note that the stability of the harmonic solution (26) depends exclusively on the exponent of coefficient $\epsilon - q$ (see Eq. (31)). Generally, if the real part of the quantity $\epsilon - q$ is negative, the variation ζ goes to zero when the time goes up and therefore, the harmonic solution (26) is stable. If it is positive, the solution is unstable and therefore, ζ never tends to zero when the time increases, but has a bounded oscillatory behavior or goes to infinity. Let us consider the two following possibilities:

- if $\epsilon = \pm\bar{\epsilon}$, then the solution for ζ can be stable if $q > 0$ and $q^2 > \epsilon^2$, otherwise it is unstable.
- if $\epsilon = \pm\mathrm{j}\bar{\epsilon}$, the solution described by Eq. (26) is stable if $q > 0$ (see Eq. (31)) and unstable if $q < 0$.

Before discussing the form of instability in the case $\epsilon = \pm\mathrm{j}\bar{\epsilon}$, let us consider the first harmonic component in the Fourier series of the function $\psi(t)$ as follows:

$$\psi(t) = \upsilon_1 \cos\Omega t + \upsilon_2 \sin\Omega t. \tag{36}$$

Consequently, the general solution for $\zeta(t)$ within the unstable region can be written as

$$\zeta(t) = \mathrm{e}^{-qt}\{\upsilon_1 \cos[(\Omega + \bar{\epsilon})t + \varphi_1] + \upsilon_2 \sin[(\Omega - \bar{\epsilon})t + \varphi_2]\}, \tag{37}$$

where υ_1, υ_2, φ_1 and φ_2 are constants. Therefore, the form of instability defined by $\epsilon = \pm\mathrm{j}\bar{\epsilon}$ (for $q < 0$) results in a build-up of new harmonic components with the frequencies $\Omega + \bar{\epsilon}$ and $\Omega - \bar{\epsilon}$, which are in general incommensurate with the frequency Ω of the periodic solution (26). Where as for $q < 0$ the solution is unstable and so that $q = 0$ is the boundary of the instability and stability region (see Fig. 4). That kind of instability can be interpreted as a Neimark instability

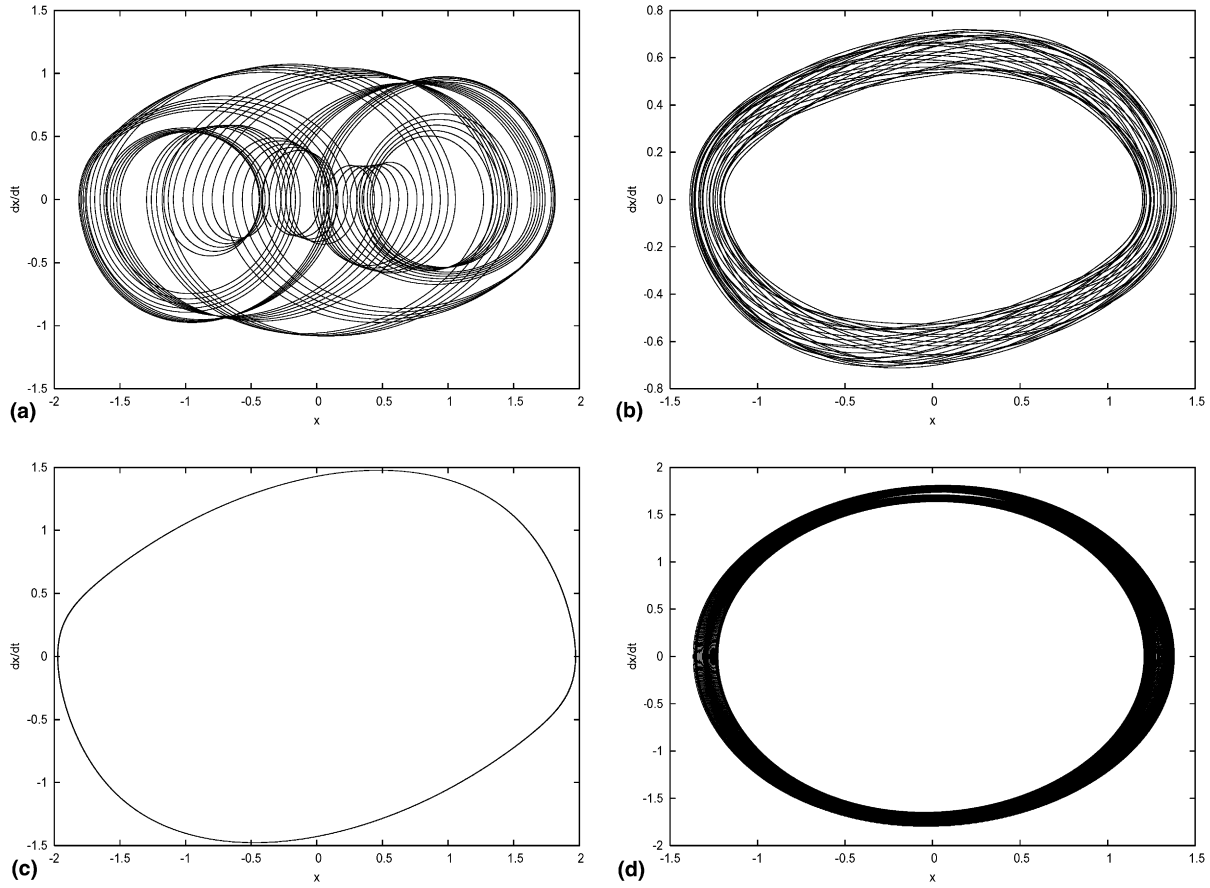

Fig. 6. Behavior of the model during the stability process with the parameters of Fig. 5 and the initial conditions $(x_0, \dot{x}_0) = (0, 0.1)$. (a) in the Neimark instability region for $\Omega = 0.30$, (b) at the first Neimark's bifurcation boundary for $\Omega = 0.474$, (c) in the region of stable oscillatory states for $\Omega = 0.70$, (d) at the second Neimark's bifurcation boundary for $\Omega = 1.33$.

which gives rise to a Neimark bifurcation. It should be noticed that the Neimark bifurcation is expected at the frequency where the stable branch of the resonance curve crosses the critical boundary $A_c = 1.282$ and in this survey, it occurs for $\Omega = 0.47$ and $\Omega = 1.33$. As we have mentioned before, the solution described by Eq. (26) is stable if $A > A_c$ and unstable if $A < A_c$. These results are observed in Fig. 4 following the comparison between analytical and numerical frequency–response curves $A(\Omega)$. The corresponding numerical critical boundary is $A_n = 1.30$ for $\Omega = 0.474$ and $\Omega = 1.331$. A very good agreement is obtained between analytical and numerical results. The behavior of the model in the Neimark instability region, at the boundary where the Neimark bifurcation occurs and in the domain of stable oscillatory states is reported in Fig. 6. Such kind of instability has been also obtained for the Van der Pol–Duffing oscillator [8].

4. Superharmonic and subharmonic oscillations

Such types of oscillations are of interest in the problem of interaction between biological systems and electromagnetic waves. Therefore, depending on the frequency of coherent electromagnetic field which should be applied in order to influence the physico-chemical basis of biological function and order, subharmonic or superharmonic frequencies can be needed. Particularly, there is a great effect of the superharmonic oscillations on the homoclinic bifurcation. Indeed, adding a superharmonic lead first to the elimination of the homoclinic bifurcation and then as a consequence, to the elimination of unwanted scattered chaotic attractors [25]. Such oscillations often occur when the frequency of the external excitation is too far or close to the natural frequency of the device. It should be stressed that harmonic,

superharmonic and subharmonic oscillations take place at different time scales. Thus the best tool to perform them is the multiple time scales method [1]. In such a case, an approximate solution is generally seeking under the form

$$x(t,\mu) = x_0(T_0,T_1) + \mu x_1(T_0,T_1) + \cdots, \tag{38}$$

where the fast scale T_0 and the slow scale T_1 are associated respectively to the unperturbated system and to the amplitude and phase modulations induced by the global first order perturbation. The time derivatives now becomes

$$\frac{\mathrm{d}}{\mathrm{d}t} = D_0 + \mu D_1 + \cdots, \qquad \frac{\mathrm{d}^2}{\mathrm{d}t^2} = D_0^2 + 2\mu D_0 D_1 + \cdots \tag{39}$$

with

$$D_0 = \frac{\partial}{\partial T_0}, \qquad D_1 = \frac{\partial}{\partial T_1}, \qquad T_n = \mu^n, \quad n = 0,1,2,\ldots.$$

Inserting expressions (38) and (39) into Eq. (9) and equating coefficients of like power of μ, one obtains

Order μ^0

$$D_0^2 x_0 + x_0 = E\cos\Omega T_0. \tag{40}$$

Order μ^1

$$D_0^2 x_1 + x_1 = -2D_0D_1x_0 + (1 - x_0^2 + \alpha x_0^4 - \beta x_0^6)D_0x_0. \tag{41}$$

After solving Eq. (40), we obtain the following general solution:

$$x_0 = A(T_1)\exp(\mathrm{j}T_0) + \Xi\exp(\mathrm{j}\Omega T_0) + \bar{A}(T_1)\exp(-\mathrm{j}T_0) + \Xi\exp(-\mathrm{j}\Omega T_0), \tag{42}$$

where $\bar{A}$ represents the complex conjugate of A and

$$\Xi = \frac{E}{2(1-\Omega^2)}.$$

Substituting the general solution x_0 into Eq. (41) yields

$$\begin{aligned} D_0^2 x_1 + x_1 = \mathrm{j}\{&\Gamma_1\exp(\mathrm{j}T_0) + \Gamma_2\exp[\mathrm{j}\Omega T_0] + \Gamma_3\exp[3\mathrm{j}\Omega T_0] + \Gamma_4\exp[\mathrm{j}(2-\Omega)T_0] + \Gamma_5\exp[3\mathrm{j}T_0] + \Gamma_6\exp[\mathrm{j}(2\\ &+\Omega)T_0] + \Gamma_7\exp[\mathrm{j}(1+2\Omega)T_0] + \Gamma_8\exp[\mathrm{j}(1-2\Omega)T_0) + \Gamma_9\exp[5\mathrm{j}T_0] + \Gamma_{10}\exp[\mathrm{j}(4+\Omega)T_0]\\ &+\Gamma_{11}\exp[\mathrm{j}(4-\Omega)T_0] + \Gamma_{12}\exp[\mathrm{j}(1+4\Omega)T_0] + \Gamma_{13}\exp(5\mathrm{j}\Omega T_0) + \Gamma_{14}\exp[\mathrm{j}(1-4\Omega)T_0]\\ &+\Gamma_{15}\exp[\mathrm{j}(2+3\Omega)T_0] + \Gamma_{16}\exp[\mathrm{j}(3+2\Omega)T_0] + \Gamma_{17}\exp[\mathrm{j}(2-3\Omega)T_0] + \Gamma_{18}\exp[\mathrm{j}(1+6\Omega)T_0]\\ &+\Gamma_{19}\exp[\mathrm{j}(3+4\Omega)T_0] + \Gamma_{20}\exp[\mathrm{j}(5-2\Omega)T_0] + \Gamma_{21}\exp[\mathrm{j}(6-\Omega)T_0] + \Gamma_{22}\exp[\mathrm{j}(3-4\Omega)T_0]\\ &+\Gamma_{23}\exp[\mathrm{j}(2+5\Omega)T_0] + \Gamma_{24}\exp[\mathrm{j}(4-5\Omega)T_0] + \Gamma_{25}\exp[\mathrm{j}(4+3\Omega)T_0] + \Gamma_{26}\exp[\mathrm{j}(3+2\Omega)T_0]\\ &+\Gamma_{27}\exp[\mathrm{j}(4-3\Omega)T_0] + \Gamma_{28}\exp[\mathrm{j}(5+2\Omega)T_0] + \Gamma_{29}\exp[\mathrm{j}(6+\Omega)T_0] + \Gamma_{30}\exp[\mathrm{j}(2-5\Omega)T_0]\\ &+\Gamma_{31}\exp[\mathrm{j}(1-6\Omega)T_0] + \Gamma_{32}\exp[7\mathrm{j}T_0] + \Gamma_{33}\exp[7\mathrm{j}\Omega T_0]\} + C\cdot C, \end{aligned} \tag{43}$$

where $C\cdot C$ denotes the complex conjugate of the previous terms while the coefficients Γ_l (l varies from 1 to 33) are given in Appendix A. Many types of resonance occur from Eq. (43) but we are focussing our analysis on two particular cases: the superharmonic and the subharmonic resonances which are displayed whenever $\Omega \approx \frac{1}{3}$ and $\Omega \approx 3$ respectively.

4.1. Superharmonic resonances

In order to express the closeness of Ω to the internal (natural) frequency, we introduce the detuning parameter σ_0 according to

$$3\Omega = 1 + \mu\sigma_0. \tag{44}$$

Thus, additionally to the terms proportional to $\exp(\pm \mathrm{j}T_0)$, the one proportional to $\exp(\pm 3\mathrm{j}\Omega T_0)$ also contribute. Therefore, the solvability condition is defined as

$$-2\frac{\mathrm{d}A}{\mathrm{d}T_1} + A - A^2\bar{A} - 2\Xi^2 A + \alpha(12A^2\bar{A}\Xi^2 + 2A^3\bar{A}^2 - 4\Omega A^2\bar{A}\Xi^2 + 6A\Xi^4) - \beta[20A\Xi^6 + (86 - 46\Omega)A^2\bar{A}\Xi^4 + 60A^3\bar{A}\Xi^2 + 5A^4\bar{A}^3] + \{\alpha\Omega(3\Xi^5 + 10A\bar{A}\Xi^3) - \Omega\Xi^3 - \beta[9\Omega\Xi^7 + 88\Omega A\bar{A}\Xi^5 + (78\Omega - A)A^2\bar{A}\Xi^3\}\exp(\mathrm{j}\sigma_0 T_1) = 0. \tag{45}$$

In polar coordinates, we let

$$A = \frac{1}{2}\rho\exp[\mathrm{j}\theta(T_1)], \tag{46}$$

where ρ and θ are real quantities and standing respectively for the amplitude and phase of the oscillator. After injecting the expression (46) into Eq. (45), we separate real and imaginary parts and it comes the two following flows:

$$\begin{aligned}\frac{\mathrm{d}\rho}{\mathrm{d}T_1} &= \varsigma_1\rho + \varsigma_2\rho^3 + \varsigma_3\rho^5 + \varsigma_4\rho^7 + (\varsigma_5 + \varsigma_6\rho^2 + \varsigma_7\rho^4)\cos\Phi,\\ \frac{\mathrm{d}\Phi}{\mathrm{d}T_1} &= \sigma_0 - \frac{\varsigma_5 + \varsigma_6\rho^2\varsigma_7\rho^4}{\rho}\sin\Phi,\end{aligned} \tag{47}$$

where

$$\varsigma_1 = \frac{1}{2} - (1 - 3\alpha\Xi^4 + 10\beta\Xi^6), \qquad \varsigma_2 = -\frac{1}{8} + \frac{1}{2}\left[\alpha(3 - \Omega) - \beta\left(\frac{43}{2} - \Omega\right)\Xi^2\right]\Xi^2, \qquad \varsigma_3 = \frac{1}{16}(\alpha - 30\beta\Xi^2),$$

$$\varsigma_4 = -\frac{5\beta}{128}, \qquad \varsigma_5 = -\Omega(1 - 3\alpha\Xi^2 + 9\beta\Xi^4)\Xi^3, \qquad \varsigma_6 = \Omega\left(\frac{5\alpha}{2} - 22\beta\Xi^2\right)\Xi^3, \qquad \varsigma_7 = \frac{\beta}{8}(2 - 39\Omega)\Xi^3,$$

$$\Phi = \sigma_0 T_1 - \theta.$$

For the steady-state motions, amplitude and phase are varied very slowly. Thus, one must have

$$\frac{\mathrm{d}\rho}{\mathrm{d}T_1} = \frac{\mathrm{d}\Phi}{\mathrm{d}T_1} = 0,$$

which corresponds to the singular points of Eq. (47) and yields

$$\begin{aligned}\varsigma_1\rho + \varsigma_2\rho^3 + \varsigma_3\rho^5 + \varsigma_4\rho^7 &= -(\varsigma_5 + \varsigma_6\rho^2 + \varsigma_7\rho^4)\cos\Phi,\\ \sigma_0\rho &= (\varsigma_5 + \varsigma_6\rho^2 + \varsigma_7\rho^4)\sin\Phi.\end{aligned} \tag{48}$$

Squaring and adding these equations give us the following nonlinear equation:

$$\varsigma_4^2\rho^{14} + 2\varsigma_3\varsigma_4 + (\varsigma_3^2 + 2\varsigma_2\varsigma_4)\rho^{10} + (2\varsigma_1\varsigma_4 + 2\varsigma_2\varsigma_4 - \varsigma_6^2)\rho^8 + (\varsigma_2^2 + 2\varsigma_1\varsigma_3 - 2\varsigma_6\varsigma_7)\rho^6 + (2\varsigma_1\varsigma_2 - 2\varsigma_5\varsigma_7 - \varsigma_6^2)\rho^4 + (\varsigma_1^2 - 2\varsigma_5\varsigma_6 + \sigma_0^2)\rho^2 - \varsigma_5^2 = 0. \tag{49}$$

Thus, the motion of the superharmonic oscillatory states is described by the following equation:

$$x(t) = \rho\cos(3\Omega t + \Phi) + \Xi\cos\Omega t + \mathrm{O}(\mu). \tag{50}$$

Eq. (49) is an implicit equation for the amplitude of the response ρ as a function of the detuning parameter σ_0 and the amplitude of the forcing term E: it is called the frequency–response equation. The Newton–Raphson algorithm is used to solve it in order to obtain the amplitude response curves $\rho(E)$ which are plotted in Figs. 7 and 8 for three different values of the parameters α and β respectively. In both cases, the hysteresis phenomenon is observed and one can notice that the parameters α and β have a real effect on the amplitude of such oscillatory states.

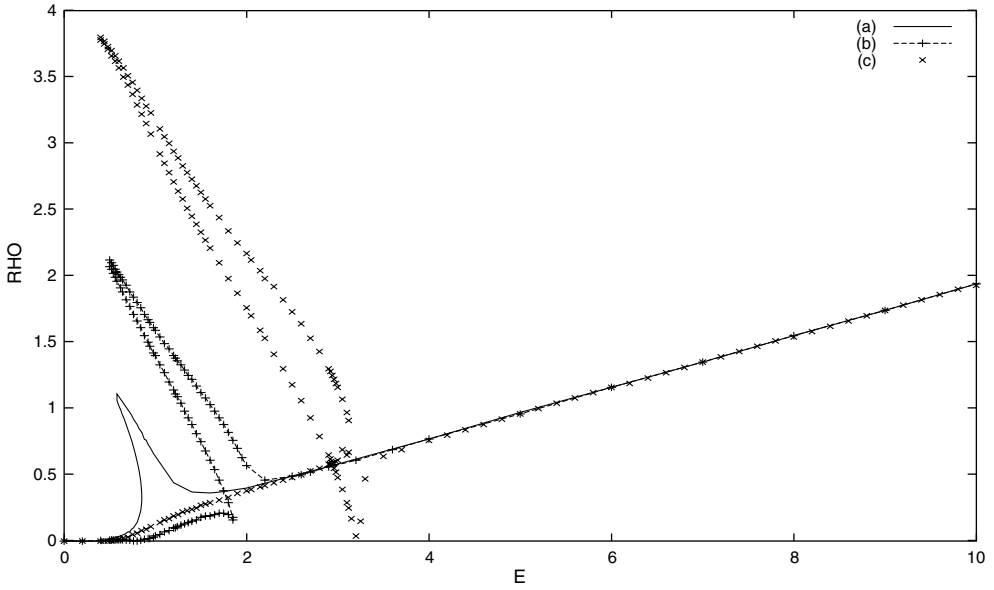

Fig. 7. Effects of the parameter α on the superharmonic amplitude–response curves for $\beta = 0.5$ and $\sigma_0 = 0.05$. (a) $\alpha = 0.1$, (b) $\alpha = 2$, (c) $\alpha = 5$.

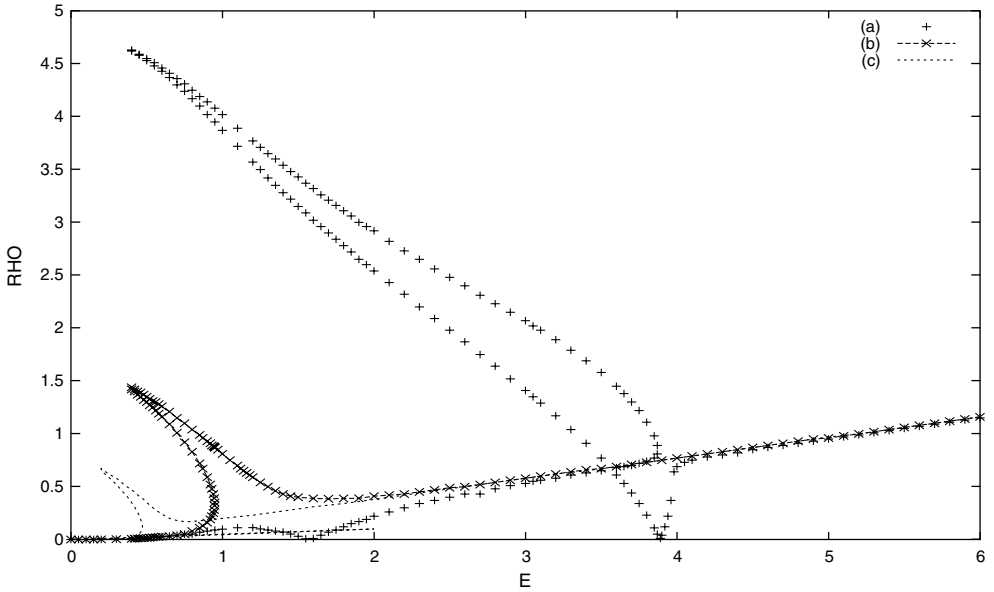

Fig. 8. Effects of the parameter β on the superharmonic amplitude–response curves for $\alpha = 0.5$ and $\sigma_0 = 0.05$. (a) $\beta = 0.03$, (b) $\beta = 0.5$, (c) $\beta = 50$.

4.2. Subharmonic resonances

To analyze the subharmonic resonances, we introduce another detuning parameter σ according to

$$\Omega = 3 + \mu\sigma. \tag{51}$$

From Eq. (43), the condition under which the secular terms are now cancelled is given by

$$-2\frac{dA}{dT_1} + A - A^2\bar{A} - 2A\Xi^2 + \alpha(12A^2\bar{A}\Xi^2 + 2A^3\bar{A}^2 - 4\Omega A^2\bar{A}\Xi + 6A\Xi^4) - \beta[20A\Xi^6 + 2(43 - 23\Omega)A^2\bar{A}\Xi^4 + 60A^3\bar{A}\Xi^2 + 5A^4\bar{A}^3] + \{(2-\Omega)\bar{A}^2\Xi - \alpha[6(2-\Omega)\bar{A}^2\Xi^3 + 4(1-\Omega)A\bar{A}^3\Xi] + \beta[30(2-\Omega)\bar{A}^2\Xi^5 + 2(56 - 27\Omega)A\bar{A}^3\Xi^3 + (26 - 15\Omega)A^2\bar{A}^4\Xi)]\}\exp(j\sigma T_1) = 0. \quad (52)$$

Once more, we introduce the polar notation (46) and after some algebraic calculations, it comes that

$$\frac{d\rho}{dT_1} = \varsigma_1\rho + \varsigma_2\rho^3 + \varsigma_3\rho^5 + \varsigma_4\rho^7 + (\widehat{\varsigma}_5\rho^2 + \widehat{\varsigma}_6\rho^4 + \widehat{\varsigma}_7\rho^6)\cos\chi,$$
$$\frac{d\chi}{dT_1} = \sigma - 3\frac{(\widehat{\varsigma}_5\rho^2 + \widehat{\varsigma}_6\rho^4 + \widehat{\varsigma}_7\rho^6)}{\rho}\sin\chi, \quad (53)$$

where

$$\widehat{\varsigma}_5 = \frac{(2-\Omega)(1-6\alpha\Xi^2)\Xi - 30\beta(\Omega+2)\Xi^5}{4}, \qquad \widehat{\varsigma}_6 = \frac{(56-27\Omega)\beta\Xi^3 - 2\alpha(1-\Omega)}{8},$$
$$\widehat{\varsigma}_7 = \frac{(26-15\Omega)\beta\Xi}{64}, \qquad \chi = \sigma T_1 - 3\theta.$$

For steady-state motions, we obtain after eliminating χ via some algebraic manipulations the following equation:

$$\rho^2\left[\varsigma_4\rho^{12} + (2\varsigma_3\varsigma_4 - \widehat{\varsigma}_7^{\,2})\rho^{10} + (\varsigma_3^2 + 2\varsigma_2\varsigma_4 - 2\widehat{\varsigma}_6\widehat{\varsigma}_7)\rho^8 + (2\varsigma_1\varsigma_4 + 2\varsigma_2\varsigma_3 - \widehat{\varsigma}_6^{\,2} - 2\widehat{\varsigma}_5\widehat{\varsigma}_7)\rho^6 + (\varsigma_2^2 + 2\varsigma_1\varsigma_3 - 2\widehat{\varsigma}_5\widehat{\varsigma}_6)\rho^4 + (2\varsigma_1\varsigma_2 - \widehat{\varsigma}_5^{\,2})\rho^2 + \varsigma_1^2 + \frac{\sigma^2}{9}\right] = 0. \quad (54)$$

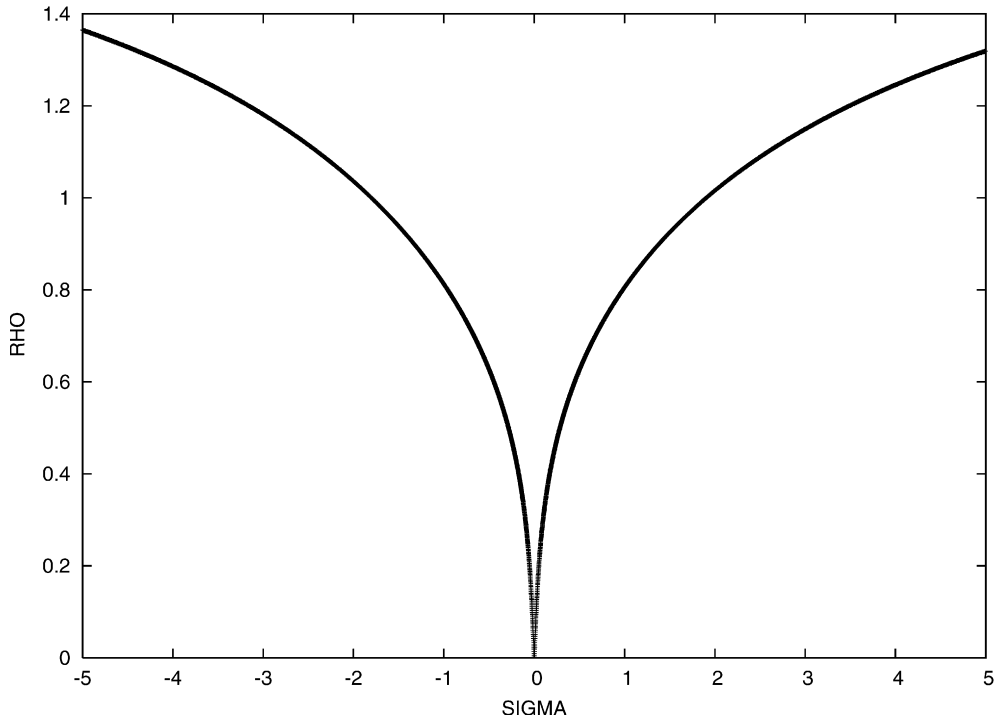

Fig. 9. Subharmonic frequency–response curves for the parameters $\alpha = 1.0$, $\beta = 0.25$, $E = 5.5$ and $\mu = 0.05$.

In this case, the motion of the subharmonic oscillatory states is described by the following equation:

$$x(t) = \rho \cos\left(\frac{\Omega}{3}t + \chi\right) + \Xi \cos \Omega t + \mathrm{O}(\mu). \tag{55}$$

The resolution of Eq. (54) using the Newton–Raphson algorithm enables us to plot in Fig. 9 the behavior of the amplitude ρ when the detuning parameter σ varies for some fixed values of the parameters α and β. Apart the harmonic, superharmonic and subharmonic oscillatory states display by the model, it can also bifurcate from the regular to the chaotic regime. Therefore, it seems very interesting to find the range of parameters for which the model switches from a regular to a chaotic oscillatory states and from a chaotic to a regular oscillation.

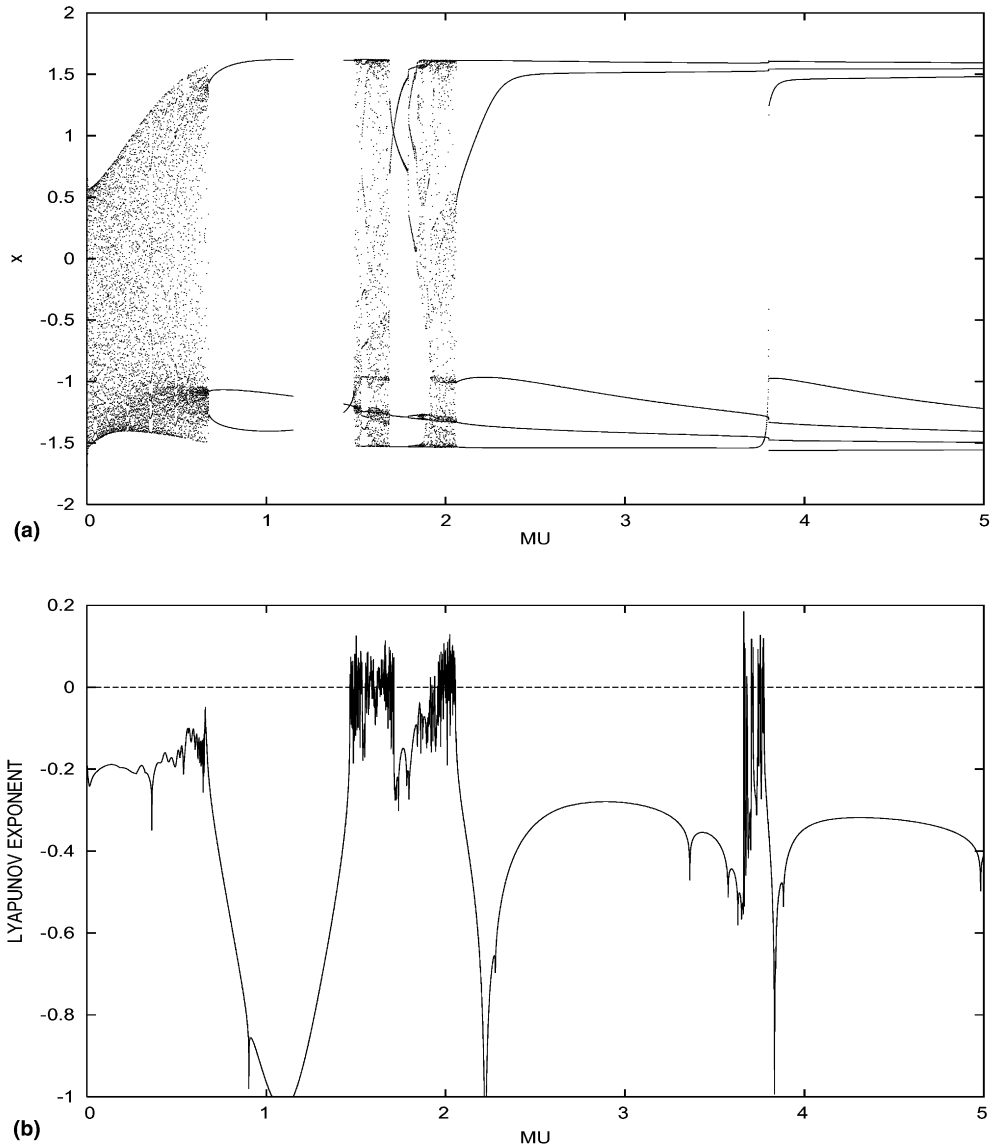

Fig. 10. Bifurcation diagram (a) and its corresponding Lyapunov exponent (b) when μ is varied with the parameters $\alpha = 2.55$, $\beta = 1.70$, $\Omega = 3.465$ and $E = 8.27$.

5. Strange attractors and transitions to chaos

As nonlinear systems, biological systems can show up regular or chaotic motions depending on some perturbation of the initial states in their environment. Thus to find the ways under which strange attractors arise in biological system is useful. Indeed, chaotic motions are of interest in executing activity adaptation and state transitions in response to environmental changes, and consequently creates a rich repertory of responses [26]. The quenching of chaos in biological systems is important in medical science because, chaos control techniques are expected to bring about new diagnostic tools and therapies for certain types of diseases, including cardiac arrhythmias [27,28] and epilepsy [29]. On the other hand, the existence of chaos is sometimes needed. Thus, the interests have been devoted in the idea that the brain may utilize transition in and out of chaos [30–32] in its processing to form a complex system [33] displaying self-organization [32], capable of generating new types of structure through bifurcation, a sudden qualitative change in structure occurring at a critical value of a continuously varying parameter. In this section, we analyze the way chaos arises in the **MLC-VdPo** described by Eq. (9). For this purpose, we solve it numerically using the Runge–Kutta algorithm and drawn the resulting bifurcation diagram and the variation of the corresponding Lyapunov exponent as the amplitude E and the coefficient μ are varied. The Lyapunov exponent is defined as

$$\mathbf{Lya} = \lim_{t\to\infty} \frac{\ln[\mathrm{d}(t)]}{t}, \tag{56}$$

with

$$\mathrm{d}(t) = \sqrt{\mathrm{d}x^2 + \mathrm{d}v_x^2},$$

where $\mathrm{d}x$ and $\mathrm{d}v_x$ are the variations of x and $\dot{x}$ respectively. The time period of the periodic stroboscopic bifurcation diagram used to map the transition is $T = \frac{2\pi}{\Omega}$. For the set of parameters $\alpha = 2.55$, $\beta = 1.70$, $\Omega = 3.465$ and $E = 8.27$, it is found that chaos appears in the system within the range of $\mu \in [1.572, 1.577] \cup [1.586, 1.588] \cup [1.937, 1.944] \cup [1.973, 1.985] \cup [1.999, 2.001] \cup [3.706, 3.709]$ as one can observe in the bifurcation diagram and its corresponding Lyapunov exponent shown in Fig. 10. Thus the phase portrait showing the chaotic behavior of the oscillator is plotted in Fig. 11 for $\mu = 2.0$. Fig. 12 presents the bifurcation diagram and the corresponding variation of the Lyapunov exponent respectively when the amplitude E is varied and the following transitions are observed. When the amplitude of the

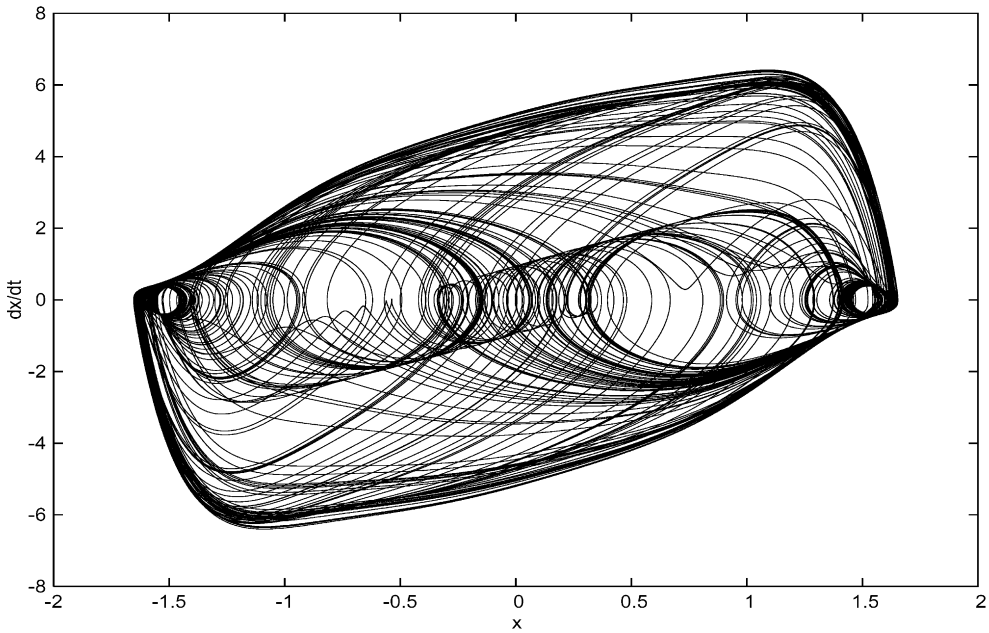

Fig. 11. Chaotic phase portrait of the model with the parameters $\alpha = 2.55$, $\beta = 1.70$, $\Omega = 3.465$, $\mu = 2.0$, $E = 8.27$ and the initial conditions $(x(0), \dot{x}(0)) = (0, 1)$.

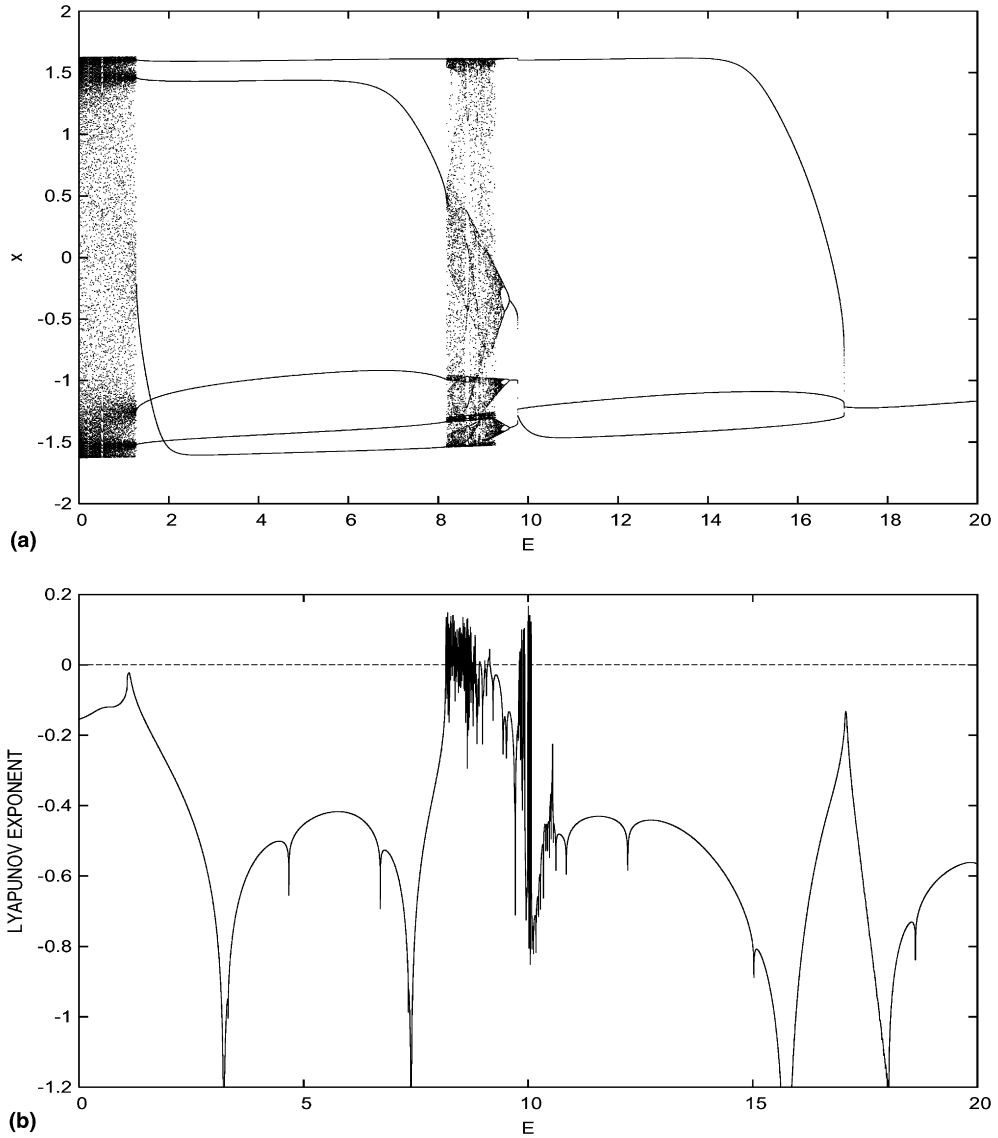

Fig. 12. Bifurcation diagram (a) and the corresponding Lyapunov exponent (b) when E varies with the parameters $\alpha = 2.55$, $\beta = 1.70$, $\Omega = 3.465$ and $\mu = 2.0$.

external excitation E increases from the value $E = 0$, the system moves from a quasiperiodic states to a period-5 orbit at $E = 1.34$. That period-5 orbit remains until $E = 8.224$ where chaos occurs with some sporadic windows of quasiperiodic orbit alternately and this persists until $E = 9.302$ where only quasiperiodic oscillations continue to be displayed. For $E = 9.50$, there is a transition from quasiperiodic behavior to a period-8 orbit. The period-8 orbit exists until $E = 9.55$ where a period-5 orbit occurs and leads to a period-4 orbit. At $E = 9.86$, once also have a transition from period-4 orbit to a small range of chaos with some sporadic windows of quasiperiodic orbit alternately and this continues to be in place until $E = 9.96$ where a period-3 orbit takes place before leading to a period-1 orbit (harmonic oscillations) at $E = 17.056$.

For another set of parameter $\alpha = 0.144$, $\beta = 0.05$, $\mu = 3.5$, $\Omega = 3.465$, $E = 11.40$ with two different sets of initial conditions, the model exhibits two particular types of chaotic attractors (see Fig. 13) which are complementary since one of the attractor can evolves toward another one through the phenomenon of degenerescence or symmetry inversion. Such type of attractors have also been reported by Leung recently in the study of the synchronization of two classical Van der Pol oscillator [19].

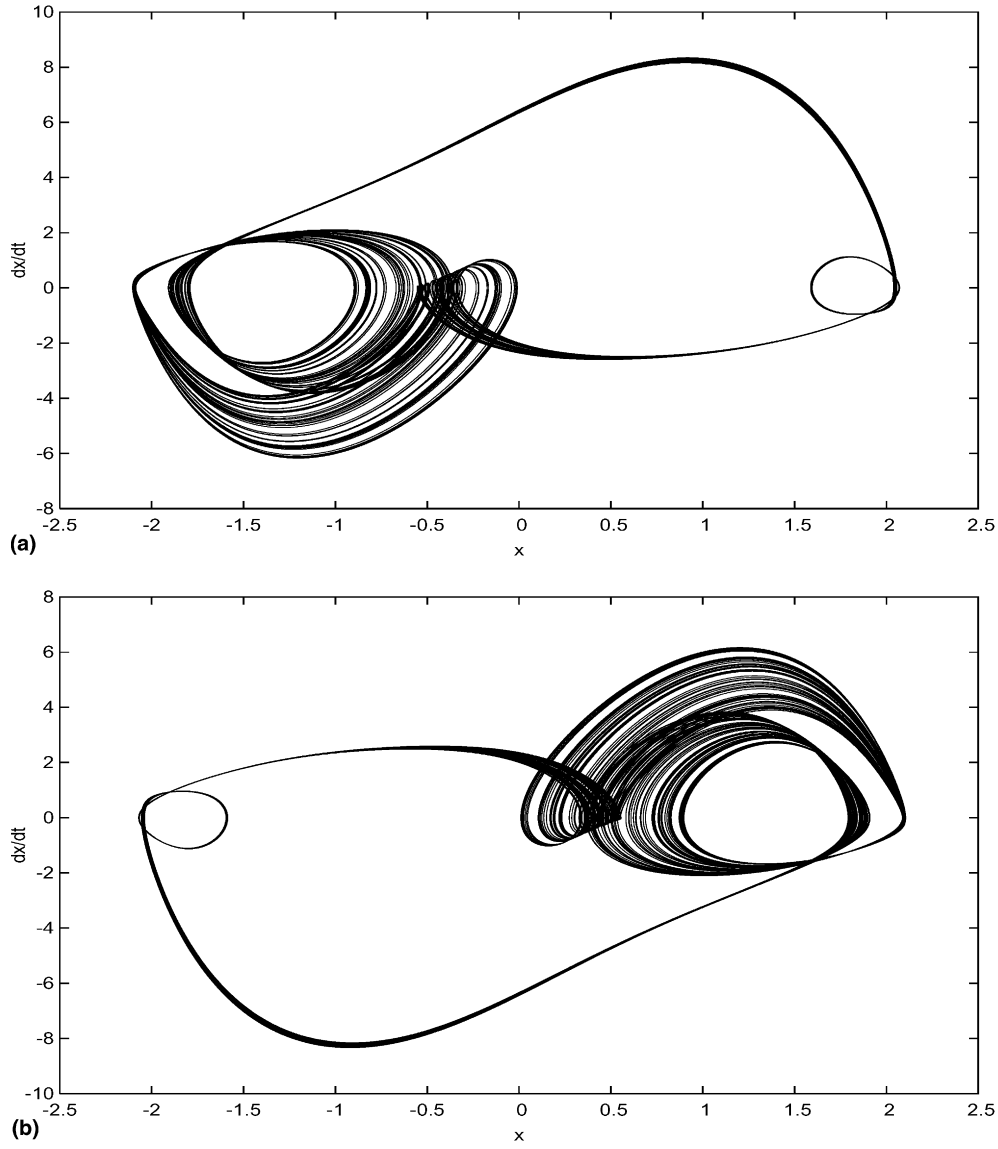

Fig. 13. Degenerated chaotic trajectories obtained for two different sets of initial conditions. (a) $(x(0), \dot{x}(0)) = (2.5, 2.5)$ (upward attractor), (b) $(u(0), \dot{u}(0)) = (3.0, 3.0)$ (downward attractor).

6. Conclusion

In this paper, we have studied the nonlinear dynamics of the biological model. A specific example of brain waves model has been used to establish the equation that governs the **MLC-VdPo**. The oscillatory states have been derived both in the non-autonomous and autonomous cases, using respectively the Lindsted's perturbation and the harmonic balance methods. The phenomenon of birhythmicity has been exhibited by the model in the autonomous regime. In the non-autonomous case, the stability boundaries of the harmonic oscillations have been derived through the Floquet theory and it has been established that the model exhibited Neimark instability. Superharmonic and subharmonic oscillatory states have been investigated also. Lyapunov exponents and bifurcation diagrams showing transitions from regular to chaotic and from chaotic to regular motions have been drawn. For a particular set of initial conditions, two degenerate chaotic attractors have been obtained. As the **MLC-VdPo** is concerned, some insights have been given for biological systems. A good comprehension of the dynamics of such a model is of importance. In biochemistry for example, the

stable limit cycles correspond to two enzymes oscillatory states. Therefore, to investigate the synchronization of such model is of interest since it possess many applications.

Appendix A

The coefficients Γ_l of Eq. (43) are the following:

$$\Gamma_1 = -2\frac{dA}{dT_1} + A - A^2\bar{A} - 2\Xi^2 A + \alpha(12A^2\bar{A}\Xi^2 + 2A^3\bar{A}^2 - 4\Omega A^2\bar{A}\Xi^2 + 6A\Xi^4) - \beta[20A\Xi^6 + (86-46\Omega)A^2\bar{A}\Xi^4 + 60A^3\bar{A}\Xi^2 + 5A^4\bar{A}^3],$$

$$\Gamma_2 = (1-2A\bar{A})\Omega\Xi - \Omega\Xi^3 + \alpha(2\Omega\Xi^5 + 14\Omega A\bar{A}\Xi^3 - 4A^2\bar{A}^2\Xi + 6\Omega A^2\bar{A}^2] - \beta[5\Omega\Xi^7 + 60\Omega A\bar{A}\Xi^5 + (186\Omega-4)A^2\bar{A}^2\Xi^3 + 20\Omega A^3\bar{A}^3],$$

$$\Gamma_3 = -\Omega\Xi^3 + \alpha\Omega(3\Xi^5 + 10A\bar{A}\Xi^3) - \beta[9\omega\Xi^7 + 88\Omega A\bar{A}\Xi^5 + (78\Omega - A)A^2\bar{A}\Xi^3],$$

$$\Gamma_4 = (\Omega-2)A^2\Xi + \alpha[6(2-\Omega)A^2\Xi^3 + 4(1-\Omega)A^3\bar{A}\Xi] - \beta[30(2-\Omega)A^2\Xi^5 + (112-54\Omega)A^3\bar{A}\Xi^3 + (26-15\Omega)A^4\bar{A}^2\Xi],$$

$$\Gamma_5 = -A^3 + \alpha[4(3+\Omega)A^3\Xi^3 + 3A^4\bar{A}] + \beta[(90+16\Omega)A^3\Xi^4 + 4(2\alpha+\Omega)A^4\bar{A}\Xi^2 + 9A^5\bar{A}^2,$$

$$\Gamma_6 = -(2+\Omega)A^2\Xi + \alpha[6(2+\Omega)A^2\Xi^3 + 4(3+\Omega)A^3\bar{A}\Xi] - \beta[4(15+38\Omega)A^2\Xi^5 + 4(53-37\Omega)A^3\bar{A}\Xi^3 + (74+15\Omega)A^4\bar{A}^2\Xi],$$

$$\Gamma_7 = -A(1+2\Omega)\Xi^2 + 4\alpha[(1+2\Omega)A\Xi^4 + (1+3\Omega)A^2\bar{A}\Xi^2] - \beta[15(1+2\Omega)A\Xi^6 + 2(85+58\Omega)A^2\bar{A}\Xi^4 + 2(61+26\Omega)A^3\bar{A}^2\Xi^2],$$

$$\Gamma_8 = -A(1-2\Omega)\Xi^2 + 4\alpha(1-2\Omega)(A\Xi^4 + A^2\bar{A}\Xi^2) - \beta[15(1-2\Omega)A\Xi^6 - 60\Omega A^2\Xi^5 + 8(22-21\Omega)A^2\bar{A}\Xi^4 + 2(64-25\Omega)A^3\bar{A}\Xi^3],$$

$$\Gamma_9 = \alpha A^5 - \beta[2(11+2\Omega)A^5\Xi^2 + 5A^6\bar{A}],$$

$$\Gamma_{10} = \alpha\Omega A^4\Xi - \beta[(40+21\Omega)A^4\Xi^3 + 2(10+3\Omega)A^5\bar{A}\Xi],$$

$$\Gamma_{11} = \alpha(4-\Omega)A^4\Xi - \beta[(56-7\Omega)A^4\Xi^3 + 2(10-3\Omega)A^5\bar{A}\Xi],$$

$$\Gamma_{12} = \alpha(1+4\Omega)A^4\Xi - \beta[6(1+4\Omega)A\Xi^6 + (19+56\Omega)A^2\bar{A}\Xi^4],$$

$$\Gamma_{13} = \alpha\Omega\Xi^5 - \beta\Omega[5\Xi^7 + 28A\bar{A}\Xi^5],$$

$$\Gamma_{14} = \alpha(1-4\Omega)A^4\Xi - \beta[6(1-4\Omega)A\Xi^6 + 7(2-26\Omega)A^2\bar{A}\Xi^4 - A^2\bar{A}],$$

$$\Gamma_{15} = 2\alpha(2+3\Omega)A^2\Xi^3 - \beta[15(2+3\Omega)A^2\Xi^5 + 4(13+11\Omega)A^3\bar{A}\Xi^3],$$

$$\Gamma_{16} = 2\alpha(3-2\Omega)A^3\Xi^2 - \beta[12(5-3\Omega)A^3\Xi^4 + 2(25-13\Omega)A^4\bar{A}\Xi^2],$$

$$\Gamma_{17} = 2\alpha(2-3\Omega)A^2\Xi^3 - \beta[2(15+7\Omega)A^2\Xi^5 + (\Omega A^2 + 32A^3\bar{A})\Xi^3],$$

$$\Gamma_{18} = -\beta[\Omega A^6\Xi + (1+6\Omega)A\Xi^6], \quad \Gamma_{19} = -\beta(9+4\Omega)A^3\Xi^4,$$

$$\Gamma_{20} = -\beta(15-6\Omega)A^5\Xi^2, \quad \Gamma_{21} = -\beta(6-\Omega)A^6\Xi,$$

$$\Gamma_{22} = \beta[(15A^4\bar{A} - A^3)\Xi^2 - 2(7-10\Omega)], \quad \Gamma_{23} = 15\Omega\beta A^4\Xi^3,$$

$$\Gamma_{24} = -\beta(6+9\Omega)A^2\Xi^5, \quad \Gamma_{25} = -\beta(4+\Omega)A^4\Xi^3,$$

$$\Gamma_{26} = -\beta[2(27+18\Omega)A^3\Xi^4 + (43+22\Omega)A^4\bar{A}\Xi^2], \quad \Gamma_{27} = 20\beta A^4\Xi^3,$$

$$\Gamma_{28} = -\beta(1+2\Omega)A^5\Xi^2, \quad \Gamma_{29} = -2\beta A^6\Xi,$$

$$\Gamma_{30} = \beta[2(3-14\Omega)A^2\Xi^5 - \Omega A^2\Xi^3], \quad \Gamma_{31} = 6\Omega\beta A\Xi^6,$$

$$\Gamma_{32} = -\beta A^7, \quad \Gamma_{33} = -\Omega\beta\Xi^7.$$

References

[1] Nayfeh AH, Mook DT. Nonlinear oscillations. New York: Wiley; 1979.
[2] Chedjou JC, Fotsin HB, Woafo P. Behavior of the Van der Pol oscillator with two external periodic forces. Phys Scr 1997;390:393–455.
[3] Van der Pol B. Philos Mag 1922;700:43, 1926;978:7–2, 1927;65:7–3, Proc. IRE 1934;1051:22.
[4] Hayashi C. Nonlinear oscillations in physical systems. New York: McGraw-Hill; 1964.
[5] Parlitz U, Lauterborn W. Period doubling cascades and devil's staircases of the driven Van der Pol oscillator. Phys Rev A 1987;1428:1434–6.
[6] Guckenheimer J, Holmes PJ. Nonlinear oscillations, dynamical systems and bifurcations of vectors fields. Berlin: Springer-Verlag; 1984.
[7] Steeb WH, Kunick A. Chaos in limit cycle systems with external periodic excitation. Int J Non-Linear Mech 1987;349:361–422.
[8] Venkatesan A, Lakshmanan M. Bifurcation and chaos in the double-well Duffing–Van der Pol oscillator: Numerical and analytical studies. Phys Rev E 1997;6321:6330–56.
[9] Hagedorn P. Non-linear oscillations. 2nd ed. Oxford: Clarendon Press; 1988.

[10] Kaiser F. Coherent oscillations in biological systems, I, Bifurcation phenomena and phase transitions in an enzyme–substrate reaction with ferroelectric behavior. Z Naturforsch A 1978;294:304–33.
[11] Frohlich H. Long range coherence and energy storage in a biological systems. Int J Quantum Chem 1968;641:649–52.
[12] Frohlich H. In: Marois, editor. Quantum mechanical concepts in biology, in theoretical physics and biology, 1969, p. 13–22.
[13] Voltera V. Lecons sur la theorie mathenatique de la lutte pour la vie. Paris: Gauthier-Villars; 1931.
[14] Kaiser F. Coherent modes in biological systems. In: Illinger KH, editor. Biological effects of nonionizing radiation. A.C.S Symp. Series, 1981, p. 157.
[15] Kaiser F. Coherent excitations in biological systems: specific effects in externally driven self-sustained oscillating biophysical systems. Berlin, Heidelberg: Springer-Verlag; 1983.
[16] Kaiser F, Eichwald C. Bifurcation structure of a driven multi-limit-cycle Van der Pol oscillator (I). The superharmonic resonance structure. Int J Bifurcat Chaos 1991;485:491–501.
[17] Eichwald C, Kaiser F. Bifurcation structure of a driven multi-limit-cycle Van der Pol oscillator (II). Int J Bifurcat Chaos 1991;711:715–21.
[18] Decroley O, Goldbeter A. Birhythmicity, chaos, and other patterns of temporal self-organization in a multiply regulated biochemical system. Proc Natl Acad Sci USA 1982;6917:6921–79.
[19] Goldbeter A, Gonze D, Houart G, Leloup JC, Halloy J, Dupont G. From simple to complex oscillatory behavior in metabolic and genetic control network. Chaos 2001;247:260–311.
[20] Goldbeter A. Biochemical oscillations and cellular rhythms: the molecular bases of periodic and chaotic behavior. Cambridge: Cambridge University Press; 1996.
[21] Kaiser F. Coherent oscillations in biological systems: interaction with extremely low frequency fields. Radio Sci 1982;17S–22S:17.
[22] Kaiser F. Theory of resonant effects of RF and MW energy. In: Grandolfo M, Michaelson SM, Rindi A, editors. Biological effects of a dosimetry of nonionizing radiation. New York: Plenum Press; 1983.
[23] Kaiser F. The role of chaos in biological systems. In: Barret TW, Pohl AH, editors. Energy transfer dynamics. Berlin: Springer; 1987.
[24] Kaiser F. Nichtlineare resonanz und chaos. Ihre relevanz fur biologische funktion. Kleinheubacher Berichte 1989;395:32.
[25] Lenci S, Rega G. Optimal numerical control of single-well to cross-well chaos transition in mechanical systems. Chaos, Solitons & Fractals 2003;173:186–215.
[26] Rabinovich MI, Abarbanel HDI. The role of chaos in neural systems. Neuroscience 1998;87(1):5–14.
[27] Garfinkel A, Spano ML, Ditto WL, Weiss JN. Controlling cardiac chaos. Science 1992;257:1320–5.
[28] Poon CS, Merrill CK. Decrease of cardiac chaos in congestive heart failure. Nature 1997;389:492–5.
[29] Schiff SJ, Jerger K, Duong DH, Chang T, Spano ML, Ditto WL. Controlling chaos in the brain. Nature 1994;370:615–20.
[30] Schuster HJ. Deterministic chaos. Berlin: Springer-Verlag; 1986.
[31] King CC. Fractal and chaotic dynamics in the brain. Progr Neurobiol 1991;279:308–36.
[32] Barton S. Chaos, self-organization and psychology. Am Psychol 1994;5:14–49.
[33] Ruthen R. Adapting to complexity. Sci Am 1993;110(January):117.